Computer Assisted Mechanics and Engineering Sciences, **10**: 149–161, 2003.

Numerical aspects of a level set based algorithm for state constrained optimal control problems[†]

Michael Hintermüller, Wolfgang Ring
Institute of Mathematics, Karl-Franzens University of Graz
Heinrichstr. 36, 8010 Graz, Austria

(Received October 25, 2002)

Numerical aspects of a level set based algorithm for state constrained linear-quadratic optimal control problems for elliptic partial differential equations are discussed. The speed function needed in the level set equation is derived from shape sensitivity analysis. The discretization operates on a fixed grid and additional boundary points representing the discrete interface between the coincidence set and the set where the bound to the state is not active. The discretization of the hyperbolic level set equation, the shape gradient of an appropriate penalty functional and an useful extension of this gradient (naturally defined only on the interface) to the whole computational domain are discussed.

1. Introduction

Many processes in engineering sciences and physics are modeled by partial differential equations. Frequently, due to technological requirements the state of the modeling system has to be kept within a certain range because otherwise the model is no longer adequate or material properties change. A typical example is given by laser surface hardening of steel [9, 10]. In [9] the following model is used

$$\begin{aligned} &\rho c_p y_t - k\Delta y = -\rho \ell a_t + u\alpha && \text{in } Q,\\ &\frac{\partial y}{\partial n} = 0 && \text{on } \Sigma,\\ &y(0) = y_0 && \text{in } \Omega. \end{aligned}$$

Hereby, ρ, c_p, k and ℓ describe the density, the heat capacity, the heat conductivity and the latent heat and are all assumed to be positive constants. The term αu represents a (volumetric) heat source due to laser radiation. Moreover, we have $Q = \Omega \times [0, T]$, the space-time domain, with a sufficiently smooth and bounded domain Ω, $T > 0$, and Σ representing its boundary. Further $a = a(y)$ is a nonlinear function with a_t the derivative with respect to time t. The state y is the temperature in the steel work-piece and must be kept strictly under the melting point. This last requirement is realized by the (hard) constraint

$$y \leq \psi - \delta \quad \text{a.e.} \qquad \text{in } Q,$$

with the melting temperature ψ and $\delta > 0$. Moreover, the laser energy u is used as a controlling quantity in order to achieve a desired material property which is realized by minimizing a target functional $J(y, u)$. Hence, we have to deal with a state-constrained nonlinear optimal control problem.

[†]This is an extended version of a paper presented at the conference *OPTY-2001, Mathematical and Engineering Aspects of Optimal Design of Materials and Structures*, Poznań, Poland, August 27–29, 2001.

A widely used numerical approach is given by sequential quadratic programming (SQP) algorithms (see e.g. [7]). The key idea is to approximate the nonlinear optimal control problem by a sequence of linear-quadratic optimal control (QP) problems which are simpler to solve and, thus, form the core part of SQP-algorithms. In the case of state constrained problems, the QP-problems inherit the state constraints from the original nonlinear problem. It is well-known [2] that state constraints are significantly more difficult to handle than control constraints or unconstrained problems. The main reason is given by poor regularity properties of so-called Lagrange multipliers.

In this note we focus on the QP-part of SQP, *i.e.* we discuss a numerical algorithm which is based on the level set methodology [11, 12] and is very well suited and efficient for linear-quadratic state constrained optimal control problems. Level set methods are well established in tracking (moving) interfaces and free boundaries (see [12] for applications). Our aim is to combine level set methods with (shape) optimization techniques in order to profit from the robustness and efficiency of level set methods and the capabilities of shape sensitivity analysis [4, 13].

The paper is organized as follows. In Section 2 we introduce a model problem and a related optimality system. Based on the new first order optimality characterization, in Section 3 a new paradigm considering the interface between the active and the inactive sets as optimization variable instead of primal and dual variables is introduced. Also problems of classical algorithmic approaches are highlighted. The new approach requires techniques from shape sensitivity analysis. Section 4 contains the algorithm, discusses many important issues of the discretization and gives a report on encouraging numerical test runs.

2. Model problem and first order optimality system

As a model QP-problem we consider the following linear-quadratic optimal control problem

$$\begin{aligned} &\min J(y,u) \\ &\text{s.t. } Ay + Bu = f \quad \text{in } \Omega, \qquad y \le \psi \quad \text{a.e. in } \Omega, \qquad (y,u) \in H_0^1(\Omega) \times L^2(\Omega), \end{aligned} \tag{1}$$

where $\Omega \subset \mathbb{R}^n$, with $n \in \{1,2,3\}$, is a bounded domain with sufficiently smooth boundary $\Sigma := \partial\Omega$. The objective functional is assumed to be convex, quadratic and radially unbounded with respect to u, and J_y can be interpreted as an element in $H^2(\Omega)$ and J_u as an element in $L^2(\Omega)$. The operator A is the self-adjoint second order linear elliptic (partial) differential operator defined as

$$Ay = \operatorname{div}(L\nabla y),$$

with

$$\begin{aligned} &L(x) = (l_{ij}(x)), \quad x \in \bar{\Omega}, \quad 1 \le i,j \le n, \quad l_{ij}(\cdot) \in C(\bar{\Omega}), \\ &(L\xi,\xi)_{\mathbb{R}^n} \ge \epsilon \|\xi\|^2_{\mathbb{R}^n} \quad \forall \xi \in \mathbb{R}^n \qquad \text{for some } \epsilon > 0. \end{aligned}$$

We further have $B \in \mathcal{L}(L^2(\Omega_U), L^2(\Omega))$, with $\Omega_U \subset \Omega$ measurable, and $f \in H^2(\Omega)$. The bound satisfies $\psi \in H^4(\Omega)$ and $0 < \psi(x) \le M$ on Σ.

It is standard to argue the existence of a unique solution $(y^*,u^*) \in H_0^1(\Omega) \times L^2(\Omega)$ of Eq. (1). Moreover, from [2] one can derive a first order optimality characterization of (y^*,u^*). In fact, (y^*,u^*) is the optimal solution of Eq. (1) if and only if there exist $p^* \in L^2(\Omega)$ and a Lagrange multiplier $\lambda^* \in \mathcal{M}(\Omega)$ satisfying

$$Ay^* + Bu^* = f \qquad \text{in } \Omega, \tag{2a}$$

$$y^* \le \psi \text{ a.e.} \qquad \text{in } \Omega, \tag{2b}$$

$$(p^*, A\phi)_\Omega + \langle \lambda^*, \phi \rangle_{\mathcal{M},C_0} = -(J_y(y^*,u^*),\phi)_\Omega \qquad \forall \phi \in H_0^1(\Omega) \cap H^2(\Omega), \tag{2c}$$

$$J_u(y^*,u^*) + B^* p^* = 0, \qquad \text{in } \Omega, \tag{2d}$$

$$\langle \lambda^*, z - y^* \rangle_{\mathcal{M},C_0} \le 0 \qquad \forall z \in C_0(\Omega) \text{ with } z \le \psi. \tag{2e}$$

Above $\mathcal{M}(\Omega)$ denotes the set of regular Borel measures, $\langle\cdot,\cdot\rangle_{\mathcal{M},C_0}$ represents the duality pairing between $C_0(\Omega)$ and its dual $\mathcal{M}(\Omega)$, and $(\cdot,\cdot)_\Omega$ is the $L^2(\Omega)$-inner product. The operator $B^\star$ denotes the adjoint of B.

Next let us define the active and inactive sets at the optimal solution, *i.e.*

$$\mathcal{A}^* := \{x \in \Omega : y^*(x) = \psi(x)\}, \qquad \mathcal{I}^* = \Omega \setminus \mathcal{A}^*.$$

It follows that $\mathcal{A}^*$ is a closed set. This is due to the fact that elliptic regularity results imply $y^* \in H^2(\Omega)$ and, thus, by the Sobolev embedding theorem $y^* \in C(\bar{\Omega})$. Let $\Gamma^* = \partial\mathcal{A}$ denote the interface between the active and inactive sets. Throughout we assume that

$$\Gamma^* = \partial\mathcal{I}^* \setminus \Sigma, \tag{A1}$$

$$\text{int}(\mathcal{A}^*) \neq \emptyset, \tag{A2}$$

$$\mathcal{I}^* \text{ and } \text{int}(\mathcal{A}^*) \text{ are sufficiently smooth.} \tag{A3}$$

A closer investigation of the properties of the optimal state and control on the interface Γ^* reveals the first order necessary and sufficient optimality conditions summarized in Theorem 1. Below, $\mathcal{W}(\mathcal{I}^*)$ is given by

$$\mathcal{W}(\mathcal{I}^*) = \{w \in L^2(\mathcal{I}^*) : A^\star w \in L^2(\mathcal{I}^*)\}.$$

By $\hat{n}$ we denote the outer unit normal to $\mathcal{I}^*$, and $n = L\hat{n}$. The jump of the normal derivative of p across Γ^* is denoted by

$$\left[\frac{\partial p}{\partial n}\right]_{\Gamma^*} = \frac{\partial p_{\mathcal{A}^*}}{\partial n_{\mathcal{A}^*}} - \frac{\partial p_{\mathcal{I}^*}}{\partial n_{\mathcal{I}^*}}$$

with $n_{\mathcal{A}^*}$ and $n_{\mathcal{I}^*} = n$ the outer normal vectors to $\mathcal{A}^*$ and $\mathcal{I}^*$, respectively. From now on we further assume that Bu^*, $B^\star p^*$ and $J_u(y^*,u^*)$ admit traces in $H^{1/2}(\Gamma^* \cup \Sigma)$.

Theorem 1 (Necessary Conditions) *Suppose $(y^*,u^*) \in H_0^1(\Omega)\times L^2(\Omega)$ is the solution of Eq. (1) and the active and inactive sets satisfy Eqs. (A1)–(A3). Then $p^* \in \mathcal{W}(\mathcal{I}^*)$, $y^* \in H^2(\Omega)$ and*

$$Ay^* + Bu^* = f \qquad \text{in } \mathcal{I}^*, \tag{3a}$$

$$A^\star p^* = -J_y(y^*,u^*) \qquad \text{in } \mathcal{I}^*, \tag{3b}$$

$$y^* < \psi \text{ in } \mathcal{I}^*, \tag{3c}$$

$$J_u(y^*,u^*) + B^\star p^* = 0, \tag{3d}$$

$$y^*_{|\Sigma} = 0, \qquad p^*_{|\Sigma} = 0, \qquad J_u(y^*,u^*)_{|\Sigma\cup\Gamma^*} = (-B^\star p^*)_{|\Sigma\cup\Gamma^*}, \tag{3e}$$

$$y^*_{|\Gamma^*} = \psi_{|\Gamma^*}, \qquad (Bu^*)_{|\Gamma^*} = (f - A\psi)_{|\Gamma^*}, \tag{3f}$$

$$\frac{\partial y^*}{\partial n}_{|\Gamma^*} = \frac{\partial \psi}{\partial n}_{|\Gamma^*}, \tag{3g}$$

$$\left[\frac{\partial p^*}{\partial n}\right]_{|\Gamma^*} \geq 0, \tag{3h}$$

$$-J_y(y^*,u^*) - A^\star p^* \geq 0 \quad \text{a.e.} \quad \text{in } \mathcal{A}^*. \tag{3i}$$

The proof of Theorem 1 is similar to the proof of the first part of Proposition 1 in [8]. The essential ingredients are the fact that the measure λ^* is concentrated on $\mathcal{A}^*$ and applications of Green's formula. Due to space restrictions we omit the proof and refer to [8].

The conditions Eq. (3) of Theorem 1 are also sufficient for (y^*,u^*) to be the unique solution to Eq. (1).

3. Traditional approaches versus a new paradigm

3.1. Problems of classical approaches

Traditional optimization techniques for computing the solution to the discretized first order optimality system (2) include projected gradient algorithms [3], projected Newton methods [3] or the primal-dual active set strategy [2]. Typically, the solution (y_h^*, u_h^*), with subscript h indicating the mesh-size of the discretization, is approximated by a sequence $\{(y_h^n, u_h^n)\}$. Every iterate induces approximations

$$\mathcal{A}_h^n = \{x \in \Omega : y_h^n(x) = \psi_h(x)\} \qquad \text{and} \qquad \mathcal{I}_h^n = \Omega \setminus \mathcal{A}_h^n,$$

of the active set $\mathcal{A}_h^*$ and the inactive set $\mathcal{I}_h^*$ and a current interface Γ_h^n. Let us take the primal-dual active set strategy (pdAS) of [2] as a model algorithm. In [2] the convergence of the finite dimensional pdAS is established. However, the measure property of λ^* is reflected in pdAS by a significant mesh dependence. In Figure 1 we display the iterates y_h^{50} and y_h^{100} for $h = 1/1000$ and a finite difference approximation. We chose L to be the identity matrix, i.e. $A = \Delta$, $\Omega_U = \Omega = (0,1)$ and B the identity operator. In our 1D-example we discretize Δ by the well-known three point stencil. It is seen that the measure property of λ^* is the reason for the peaks in λ_h^n. We further observe in our test runs that in the estimates of the active and inactive sets only two pixels are corrected from one iteration to the next. This results in a significant dependence of the number of iterations of pdAS on the mesh-size of discretization. This behavior is also typical for e.g. projected Newton methods. In fact, these algorithms admit no analysis in function spaces.

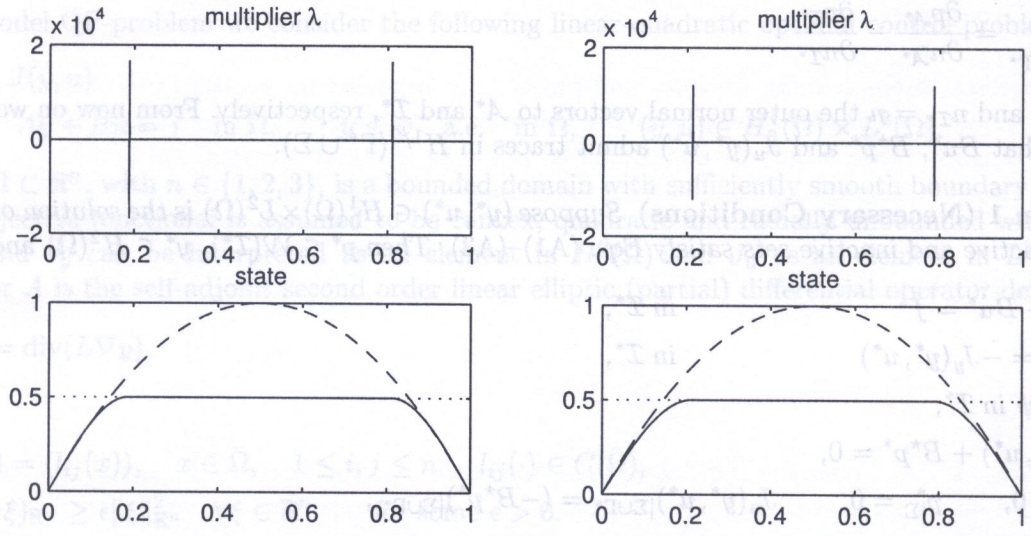

Fig. 1. Multiplier and state iterates at iteration 50 (left) and 100 (right); bound ψ (dotted), y_d (dashed)

3.2. Free boundary perspective

In order to circumvent the problems described above, we propose a different concept. Instead of considering the primal and dual variables y, u, p, λ as the optimization variables, by relaxing some of the interface conditions we interpret Eq. (3) as a free boundary problem which allows us to consider the interface Γ as the optimization variable. Since the correct active and inactive sets are not known a priori, we have to update the geometry iteratively. Here we utilize the fact that the interface Γ^* uniquely defines $\mathcal{A}^*$ and $\mathcal{I}^*$. In fact, we consider the approximations Γ^n of Γ^* as discrete snapshots of a continuously moving geometry that defines current approximations $\mathcal{A}^n$ and $\mathcal{I}^n$. The violation of

the relaxed interface conditions together with the possible violation of the bound constraint $y \leq \psi$ is taken care of by a penalty functional $P(\Gamma) \geq 0$. At the optimal geometric configuration we have $P(\Gamma^*) = 0$, and as long as at least one of the conditions is violated at Γ^n we have $P(\Gamma^n) > 0$. Thus, we aim to minimize $P(\Gamma)$. This requires shape sensitivity analysis in the spirit of [4, 13]. If we relax Eqs. (3c), (3g), (3h) and realize (3i) by the initial choice Γ^0, we have

$$P(\Gamma) = \frac{1}{2|\Gamma|} \int_\Gamma \left(\left| \frac{\partial}{\partial n}(y - \psi) \right|^2 + c_1 \left(\max\left(0, -\left[\frac{\partial}{\partial n} p\right]_\Gamma\right)\right)^2 \right) \mathrm{d}\Gamma$$

$$+ \frac{c_2}{2} \int_{\mathcal{I}} (\max(0, y - \psi))^2 \, \mathrm{d}x, \tag{4}$$

where $c_1, c_2 > 0$ denote penalty parameters. The factor $\frac{1}{|\Gamma|}$ prevents the penalty functional from vanishing due to vanishing $|\Gamma|$. Note that $y = y(\Gamma)$ and $p = p(\Gamma)$ due to

$$Ay + Bu = f \qquad \text{in } \mathcal{I}, \tag{5a}$$

$$A^\star p = -J_y(y, u) \qquad \text{in } \mathcal{I}, \tag{5b}$$

$$J_u(y^*, u^*) + B^\star p^* = 0, \tag{5c}$$

$$y_{|\Sigma} = 0, \qquad p_{|\Sigma} = 0, \qquad J_u(y, u)_{|\Sigma \cup \Gamma} = (-B^\star p)_{|\Sigma \cup \Gamma}, \tag{5d}$$

$$y_{|\Gamma} = \psi_{|\Gamma}, \qquad (Bu)_{|\Gamma} = (f - A\psi)_{|\Gamma}, \tag{5e}$$

with $\mathcal{A}$ and $\mathcal{I}$ induced by Γ.

In order to ease the subsequent discussion from technicalities, from now on we assume that $\Omega_U = \Omega$, $B = I$, and

$$J(y, u) = \frac{1}{2}\|y - y_d\|^2_{L^2(\Omega)} + \frac{\alpha}{2}\|u\|^2_{L^2(\Omega)},$$

with $y_d \in H^2(\Omega)$ and $\alpha > 0$. Thus, we can eliminate p due to

$$-\alpha u = p$$

by Eq. (5c) and the third condition in Eq. (5d).

Concerning the solvability of Eq. (5) we have the following result.

Proposition 1. *Suppose that the open set $\mathcal{I} \subset \Omega$ satisfies $\Sigma \subset \mathcal{I}$, $\Gamma = \partial\mathcal{I} \setminus \Sigma \neq \emptyset$ and Eqs.* (A1)–(A3). *Then Eq.* (5) *admits a unique solution $(y, u) \in H^2(\mathcal{I}) \times H^2(\mathcal{I})$.*

Proof. Note that due to our assumptions Eq. (5) becomes

$$Ay + u = f \qquad \text{in } \mathcal{I}, \tag{6a}$$

$$y - \alpha A^\star u = y_d \qquad \text{in } \mathcal{I}, \tag{6b}$$

$$y_{|\Sigma} = 0, \qquad u_{|\Sigma} = 0, \tag{6c}$$

$$y_{|\Gamma} = \psi_{|\Gamma}, \qquad u_{|\Gamma} = (f - A\psi)_{|\Gamma}. \tag{6d}$$

It is straightforward to transform this system into a system with homogeneous Dirichlet boundary conditions on $\partial\mathcal{I}$ and modified right hand sides. Using the first equation, the state y can be expressed by

$$y = A^{-1}(-u + f_1)$$

where f_1 denotes some appropriate right hand side due to the transformation of the boundary conditions and

$$A^{-1} : L^2(\mathcal{I}) \to H^2(\mathcal{I}) \cap H^1_0(\mathcal{I})$$

is the solution operator to the homogeneous Dirichlet problem for A on $\mathcal{I}$. Utilizing the second equation we obtain

$$A^{-1}u + \alpha A^{\star}u = f_2 \quad \text{on } \mathcal{I},$$

with an appropriate f_2. It is straightforward to show that this equation admits a unique solution in $H^2(\mathcal{I})$. This completes the proof. □

Proposition 1 guarantees that our free boundary perspective is a well-defined concept.

3.3. Level set aspect and shape sensitivity

Now we clarify how the geometry is propagated such that $P(\Gamma)$ tends to zero. Following the level set idea due to Osher and Sethian [11] we assume that the current interface $\Gamma(t)$[1] is the zero level set of an oriented distance function $\phi : [0,\infty) \times \Omega \to \mathbb{R}$. Further we suppose that the interface evolves along $-\hat{F}n$, where $-\hat{F}$ defines a so-called speed (or velocity) function. We require that a particle on the interface with path $x(t)$ must always be zero, *i.e.*

$$\phi(t, x(t)) = 0.$$

By the chain rule we have

$$\phi_t + \nabla\phi \cdot x'(t) = 0.$$

Since the interface evolves along $-\hat{F}n$ and $n = \nabla\phi/|\nabla\phi|$ (this follows from the fact that ϕ is an oriented distance function), we obtain

$$\phi_t - \hat{F}|\nabla\phi| = 0, \qquad \phi(0,\cdot) = \phi_0\,,$$

the *level set equation* [12]. Observe that whenever $\hat{F} \equiv 0$, then a stationary solution is reached and the interface remains unchanged in time.

In order to define $\hat{F}$ appropriately, we introduce the Eulerian derivative of $P(\Gamma)$ with respect to Γ in direction of an admissible vector field V [13]

$$\mathrm{d}P(\Gamma; V) = \lim_{t \downarrow 0} \frac{1}{t}(P(\Gamma_t) - P(\Gamma_0)),$$

where $\Gamma_t = T_t(\Gamma)$ and $\Gamma_0 = \Gamma$. Here T_t denotes the time-t map defined in [13]. It is known [13, Thm. 2.27] that under suitable assumptions there exists a distribution F on Γ such that

$$\mathrm{d}P(\Gamma; V) = \langle F, v_n \rangle_\Gamma, \quad \text{with } v_n = V(0,x) \cdot n(x).$$

Hence, we utilize the negative gradient $-F$ in defining the speed function in the level set equation[2]. At Γ^*, the interface at the optimal solution of Eq. (1), we have

$$\mathrm{d}P(\Gamma^*; V) = 0 \quad \text{for all admissible vector fields } V.$$

Utilizing the shape sensitivity calculus provided in the monograph by Sokolowski and Zolesio [13] we obtain the following result.

[1] The notation $\Gamma(t)$ reflects the idea that the geometry is continuously moving.

[2] Note that F is defined on Γ, while $\hat{F}$ is defined on Ω. $\hat{F}$ is obtained from F by an extension technique.

Theorem 2. *Under appropriate regularity assumptions the Eulerian derivative of P is given by*

$$\begin{aligned} \mathrm{d}P(\Gamma;V) = &\int_\Gamma \left(\alpha \frac{\partial \mu}{\partial n}\frac{\partial}{\partial n}(u+\Delta\psi) - \frac{\partial \nu}{\partial n}\frac{\partial}{\partial n}(y-\psi)\right) v_n \,\mathrm{d}\Gamma \\ &+ \frac{c_1}{|\Gamma|}\int_\Gamma m'\left(\frac{\partial}{\partial n}(u+\Delta\psi)\right)(\alpha^{-1}(y-y_d)+\Delta^2\psi)v_n \,\mathrm{d}\Gamma \\ &- \frac{1}{|\Gamma|}\int_\Gamma \kappa\left(\frac{1}{2}\left|\frac{\partial}{\partial n}(y-\psi)\right|^2 + c_1 m\left(\frac{\partial}{\partial n}(u+\Delta\psi)\right)\right) v_n \,d\Gamma \\ &- \frac{1}{|\Gamma|^2}\int_\Gamma \kappa v_n \,\mathrm{d}\Gamma \cdot \left(\int_\Gamma \left(\frac{1}{2}\left|\frac{\partial}{\partial n}(y-\psi)\right|^2 + c_1 m\left(\frac{\partial}{\partial n}(u+\Delta\psi)\right)\right)\mathrm{d}\Gamma\right), \end{aligned}$$

where (μ,ν) solves the adjoint problem

$$\begin{aligned} &\Delta\nu + \mu = c_2 m'(y-\psi) && \text{in } \mathcal{I}, \\ &\nu - \alpha\Delta\mu = 0 && \text{in } \mathcal{I}, \\ &\mu_{|\Sigma} = 0, \qquad \nu_{|\Sigma} = 0, \\ &\nu_{|\Gamma} = \frac{1}{|\Gamma|}\frac{\partial}{\partial n}(y-\psi)_{|\Gamma}, \\ &\mu_{|\Gamma} = -\frac{c_1}{\alpha|\Gamma|} m'\left(\frac{\partial}{\partial n}(u+\Delta\psi)\right)_{|\Gamma}. \end{aligned}$$

Further $m(x) = \frac{1}{2}\max(0,x)^2$, κ is the mean curvature, and $v_n = V(0)n$ on Γ.

For the proof of Theorem 2 and for regularity properties of the shape and material derivatives of (y,u) we refer to [8].

Theorem 2 implies that $Fn = \nabla_\Gamma P$ with

$$\begin{aligned} \nabla_\Gamma P(\Gamma) = \Bigg[&\alpha \frac{\partial \mu}{\partial n}\frac{\partial}{\partial n}(u+\Delta\psi) - \frac{\partial \nu}{\partial n}\frac{\partial}{\partial n}(y-\psi) \\ &+ \frac{c_1}{|\Gamma|} m'\left(\frac{\partial}{\partial n}(u+\Delta\psi)\right)(\alpha^{-1}(y-y_d)+\Delta^2\psi) \\ &- \frac{1}{|\Gamma|}\kappa\left(\frac{1}{2}\left|\frac{\partial}{\partial n}(y-\psi)\right|^2 + c_1 m\left(\frac{\partial}{\partial n}(u+\Delta\psi)\right)\right) \\ &- \frac{\kappa}{|\Gamma|^2}\cdot\left(\int_\Gamma \left(\frac{1}{2}\left|\frac{\partial}{\partial n}(y-\psi)\right|^2 + c_1 m\left(\frac{\partial}{\partial n}(u+\Delta\psi)\right)\right)\mathrm{d}\Gamma\right)\Bigg] n. \end{aligned}$$

4. Algorithm and numerical aspects

4.1. The algorithm

Now we have all ingredients to define the level set based algorithm for solving the state constrained problem (1).

Level set based algorithm

(0) Choose a feasible initial Γ^0 (closed curve). Initialize ϕ^0 to be the oriented distance function with respect to Γ^0; $n := 0$.

(1) Compute (y^n, u^n) from Eq. (6) at $(\mathcal{I}^n, \Gamma^n)$.

(2) Evaluate $P(\Gamma^n)$ and compute $\nabla_\Gamma P(\Gamma^n)$. If $\nabla_\Gamma P(\Gamma^n)$ vanishes then stop; otherwise continue with step (3).

(3) Compute an appropriate extension of $\nabla_\Gamma P(\Gamma^n)$ to Ω.

(4) Use the extension of step (3) in the level set equation. Perform a time step to obtain ϕ^{n+1}, the update of ϕ^n. Set Γ^{n+1} to the zero level set of ϕ^{n+1} and put $n := n+1$. Go to step (1).

The initial choice in step (0) is called feasible if the active set $\mathcal{A}^0$ induced by Γ^0 satisfies

$$\mathcal{A}^0 \subset \mathcal{M} := \{x \in \Omega : y_d - \psi - \alpha\Delta^2\psi \geq 0\};$$

compare Eq. (3i). In our numerical tests we typically have $\mathcal{A}^n \subset \mathcal{M}$ for all $n \geq 1$.

4.2. Discretization issues

When discretizing the above algorithm special care must be taken in discretizing the level set equation and in computing the shape derivative of P. Note that the level set equation is a Hamilton–Jacobi type hyperbolic equation. For its discretization we use an ENO-scheme due to [6]; see also [12]. This scheme is second order accurate in space and is defined in 2D by

$$\phi_{ij}^{n+1} = \phi_{ij}^n - \Delta t \left[\max(\hat{F}_{ij}, 0)\nabla^+ + \min(\hat{F}_{ij}, 0)\nabla^-\right] \tag{7}$$

with

$$\nabla^+ = \left[\max(A,0)^2 + \min(B,0)^2 + \max(C,0)^2 + \min(D,0)^2\right]^{1/2},$$

$$\nabla^- = \left[\max(B,0)^2 + \min(A,0)^2 + \max(D,0)^2 + \min(C,0)^2\right]^{1/2},$$

and

$$A = D_{ij}^{-x} + \frac{\Delta x}{2}\, s(D_{ij}^{-x-x}, D_{ij}^{+x-x}),$$

$$B = D_{ij}^{+x} - \frac{\Delta x}{2}\, s(D_{ij}^{+x+x}, D_{ij}^{+x-x}),$$

$$C = D_{ij}^{-y} + \frac{\Delta y}{2}\, s(D_{ij}^{-y-y}, D_{ij}^{+y-y}),$$

$$D = D_{ij}^{+y} - \frac{\Delta y}{2}\, s(D_{ij}^{+y+y}, D_{ij}^{+y-y}).$$

Obviously, we use a finite difference discretization which is explicit in time. The subscripts i, j refer to points x_{ij} on the grid. The short hand notation D_{ij}^{+x} refers to a forward difference approximation $D_{ij}^{+x} = (\phi_{i+1,j} - \phi_{ij})/\Delta x$. Analogously one defines the backward difference D_{ij}^{-x} in the x-direction and forward and backward differences in the y-direction. The switch function s is given by

$$s(x,y) = \begin{cases} \left\{ \begin{array}{ll} x & \text{if } |x| \leq |y| \\ y & \text{if } |x| > |y| \end{array} \right\} & xy \geq 0, \\ 0 & xy < 0. \end{cases}$$

Usage of first order upwind schemes is not adequate due to a remarkable lack of accuracy in computing the zero level set; see Fig. 4. Also the accuracy in the solutions of Eq. (5) and the adjoint problem deteriorates which has its impact in computing the shape gradient.

The convergence speed of the algorithm depends also on the time step-size Δt. From the stability analysis of first order upwind schemes it is known that Δt must satisfy the CFL-condition [5, Thm. 7.7]

$$\|\hat{F}\|_\infty \Delta t \leq h,$$

where we assume a uniform grid with $h = \Delta x = \Delta y$. Especially in early stages of the iteration of our new level set based algorithm, the CFL-condition yields rather small time-step sizes. For the extra cost of a re-initialization of ϕ (which will be discussed subsequently) one can choose much larger step-sizes resulting in a rapidly converging algorithm. Also the dependence of the discretization on the space step-size is significantly relaxed. As control criterion for the time step-size we use the Armijo-type condition

$$P(\Gamma^n(\Delta t)) - P(\Gamma^n) \leq -\gamma \Delta t^n \|\nabla_\Gamma P(\Gamma^n)\|^2, \qquad \text{with } 0 < \gamma < \frac{1}{2}, \tag{8}$$

with an appropriate norm $\|\cdot\|$. Here, $\Gamma^n(\Delta t)$ refers to the zero level set of the oriented distance function obtained from Eq. (7) with time step Δt. If Eq. (8) is not satisfied, then Δt is reduced to a smaller value Δt, the new $P(\Gamma^n(\Delta t))$ is computed and Eq. (8) is tested again. As soon as Eq. (8) is satisfied or $\Delta t < \Delta t_{CFL}$ the step and the new zero level set are accepted, and ϕ^{n+1} is computed. Here Δt_{CFL} refers to the time step-size obtained from the CFL-condition.

Next we clarify how to initialize Γ^0 and how to re-initialize at the end of step (4)[3]. An idea due to [14] is to choose an estimate $\hat{\phi}^0$ of ϕ^0 such that $\hat{\phi}^0_{|\Gamma^0} = 0$ and $\hat{\phi}^0 > 0$ outside the closed curve Γ^0 and $\hat{\phi}^0 < 0$ inside. Then one considers

$$\phi_t = \operatorname{sign}(\hat{\phi}^0)(1 - |\nabla \phi|)$$

which is iterated until a steady state is reached. Then the steady state solution is ϕ^0. In our computations we use a regularization of the sign-function, *i.e.*

$$\operatorname{sign}_\epsilon(\phi) = \frac{\phi}{\sqrt{\phi^2 + \epsilon^2}},$$

with some small $\epsilon > 0$. For the re-initialization we use the same technique. But now $\hat{\phi}^0$ is replaced by ϕ^{n+1}. The re-initialization takes place at the end of step (4).

Now we briefly explain how $P(\Gamma)$ and $\nabla_\Gamma P(\Gamma)$ are computed. First we introduce several types of grid points: interior inactive points, boundary inactive points, boundary points and active points. For the respective meaning we refer to Fig. 2. A boundary point x^b_{ij} is defined by $\bar{\phi}_h(x^h_{ij}) = 0$ on the grid, *i.e.* one grid neighbor is an active point and the other one is inactive. By $\bar{\phi}_h$ we denote the linear interpolation of ϕ^n_h, the discrete approximation of ϕ^n defined on the grid points. The set of boundary points defines the discrete approximation of Γ^n. Note that we essentially work on a fixed grid (!) and only add boundary points for obtaining a good approximation of the discrete interface. The approximation of $P(\Gamma)$ is computed in the following way: The integral over $\mathcal{I}$ is approximated by the trapezoidal rule on a grid shifted by $h/2$ and involves only interior inactive points. For the approximation of the first integral over Γ we exploit the fact

$$\frac{\partial}{\partial n}(y - \psi)n = \nabla(y - \psi).$$

[3] In the subsequent discussion we dismiss the iteration index n.

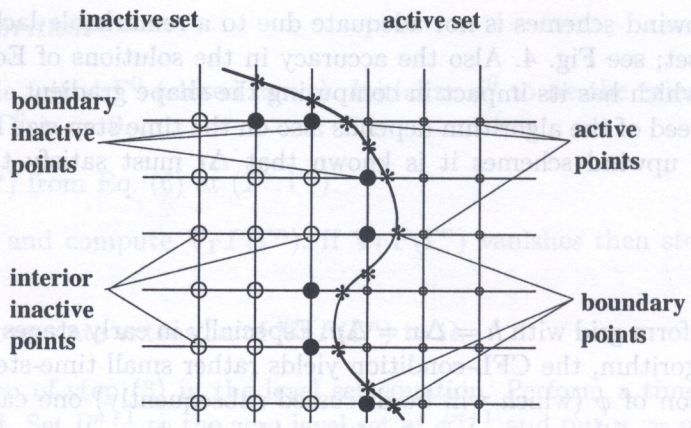

Fig. 2. Types of grid points

For its theoretical foundation we refer to [8]. A central difference approximation of the gradient is computed on the fixed grid points. In order to obtain the approximation on boundary points, we take the gradient approximation on the closest interior inactive point. The approximation of the second integral over Γ is more difficult since we have to specify a sign of the normal derivative of $u + \Delta\psi$. We determine the sign at a boundary point by the difference between the boundary point and its closest interior inactive point. The normal derivative can again be replaced by the gradient approximation like above. Finally, $|\Gamma|$ is computed in a cell oriented manner, *i.e.* all cells intersecting the zero level set are determined and the interface in a cell is approximated by a line segment. The length of these segments is summed up to obtain an approximation of $|\Gamma|$.

Many of the techniques for computing an approximation to $P(\Gamma)$ are again utilized when computing $\nabla_\Gamma P$. The mean curvature (in 2D)

$$\kappa = \nabla \cdot \frac{\nabla\phi}{|\nabla\phi|} = \frac{\phi_{xx}\phi_y^2 - 2\phi_y\phi_x\phi_{xy} + \phi_{yy}\phi_x^2}{(\phi_x^2 + \phi_y^2)^{3/2}}$$

is approximated by using central differences on the fixed grid for each of the partial derivatives of ϕ displayed above.

Finally, we explain the extension technique, *i.e.* the procedure for extending $\nabla_\Gamma P(\Gamma)$ to the whole domain Ω. The main aim is to use a construction such that the oriented distance function character of ϕ is preserved when performing a time step in the level set equation. Let us assume that we have $|\nabla\phi(t = 0, x)| = 1$ and we move under the level set equation. Then we infer formally (see also [12])

$$\frac{\mathrm{d}|\nabla\phi|^2}{\mathrm{d}t} = \frac{\mathrm{d}}{\mathrm{d}t}(\nabla\phi \cdot \nabla\phi) = 2\nabla\phi \cdot \frac{\mathrm{d}}{\mathrm{d}t}\nabla\phi = 2\nabla\phi \cdot \nabla\hat{F}|\nabla\phi| + 2\nabla\phi \cdot \nabla|\nabla\phi|\hat{F}. \tag{9}$$

Thus, if

$$\nabla\phi \cdot \nabla\hat{F} = 0 \tag{10}$$

then the right hand side in Eq. (9) vanishes and, thus, the oriented distance character of ϕ is preserved. Therefore, we use the condition (10) for computing the extension velocity $\hat{F}$ from $\nabla_\Gamma P(\Gamma)$. The algorithm we use is similar to the one in [1].

4.3. Numerical results

Now we discuss some numerical results attained by an implementation of the level set based algorithm.

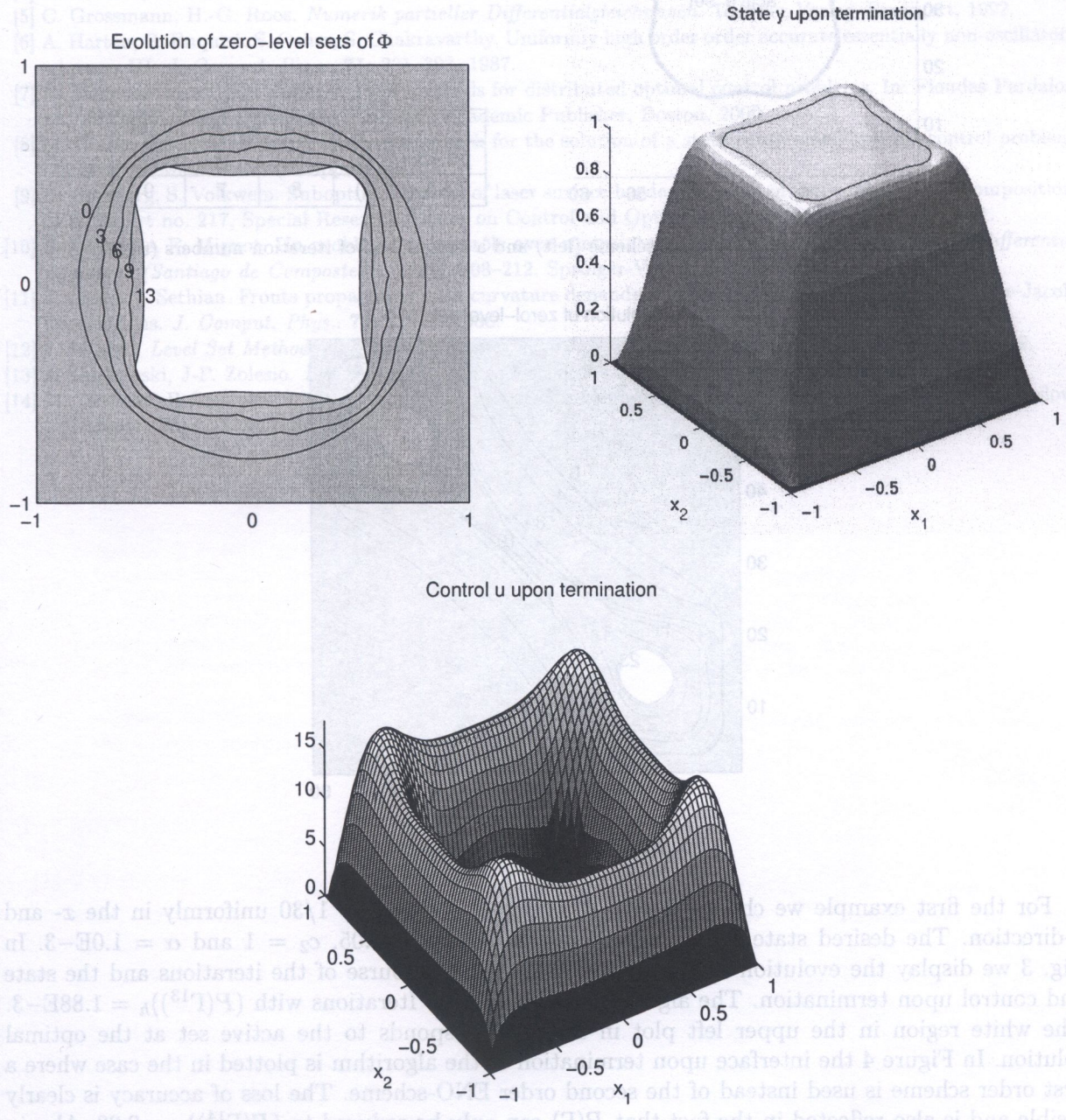

Fig. 3. Evolution of the zero level sets in the course of the iterations (upper left) and the state (upper right) and control (lower) upon termination

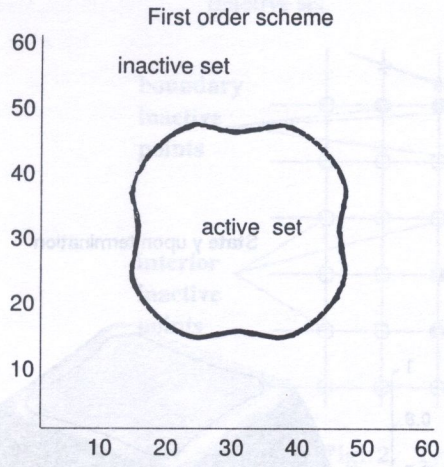

h	1/30	1/45	1/60
pdAS (# it)	11	16	21
LSA (# it)	8	7	9

Fig. 4. Interface for a first order scheme (left) and a comparison of iteration numbers (right)

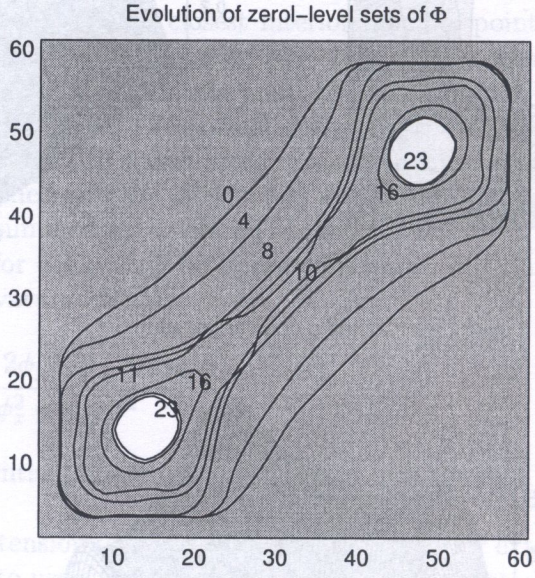

Fig. 5. Topology change.

For the first example we choose $\Omega = (-1,1)^2$, $\psi \equiv 1$ and $h = 1/30$ uniformly in the x- and y-direction. The desired state y_d is chosen as $y_d \equiv 1.2$, $c_1 = 0.05$, $c_2 = 1$ and $\alpha = 1.0\text{E}{-3}$. In Fig. 3 we display the evolution of the zero level sets in the course of the iterations and the state and control upon termination. The algorithm stops after 13 Iterations with $(P(\Gamma^{13}))_h = 1.88\text{E}{-3}$. The white region in the upper left plot in Fig. 3 corresponds to the active set at the optimal solution. In Figure 4 the interface upon termination of the algorithm is plotted in the case where a first order scheme is used instead of the second order ENO-scheme. The loss of accuracy is clearly visible and is also reflected in the fact that $P(\Gamma)$ can only be reduced to $(P(\Gamma^{14}))_h = 0.08$. Also in Fig. 4 a comparison with respect to the dependence of the number of iterations on the mesh-size of discretization between pdAS of [2] and our level set based algorithm is displayed. For our new algorithm we use now a more progressive choice for the time step-size than in the previous run. Still Eq. (8) is used as the controlling mechanism. We see that pdAS significantly depends on the mesh-size, while the level set based algorithm (LSA) is almost mesh-independent.

The new algorithm is also capable of dealing with topology changes in the course of the iteration. In Fig. 5 we only display the evolution of the zero level set. Again the white regions correspond to the active set upon termination of the algorithm. For more details we refer to [8].

REFERENCES

[1] D. Adalsteinsson, J. Sethian. The fast construction of extension velocities in level set methods. *J. Comput. Phys.*. **148**: 2–22, 1999.

[2] M. Bergounioux, K. Kunisch. Primal-dual strategy for state constrained optimal control problems. *Computational Optimization and Applications*, to appear.

[3] D. Bertsekas. *Nonlinear Programming.* Athena Scientific Publisher, Belmont, Massachusetts, 1995.

[4] M. Delfour, J.-P. Zolesio. *Shapes and Geometries.* SIAM, Philadelphia, 2001.

[5] C. Grossmann, H.-G. Roos. *Numerik partieller Differentialgleichungen.* Teubner-Verlag, Stuttgart, 1992.

[6] A. Harten, B. Enquist, S. Osher, S. Chakravarthy. Uniformly high order order accurate essentially non-oscillatory schemes; III. *J. Comput. Phys.*, **71**: 231–303, 1987.

[7] M. Heinkenschloss. SQP interior point methods for distributed optimal control problems. In: Floudas Pardalos, ed., *Encyclopedia of Optimization.* Kluwer Academic Publisher, Boston, 2000.

[8] M. Hintermüller, W. Ring. A level set approach for the solution of a state constrained optimal control problem. *Numerische Mathematik* (to appear).

[9] D. Hömberg, S. Volkwein. Suboptimal control of laser surface hardening using proper orthogonal decomposition. SFB-Report no. 217, Special Research Center on Control and Optimization, University of Graz, 2001.

[10] E. Lunéville, F. Mignot. Un problème de contrôle avec contraintes sur l'etat. In: *Control of Partial Differential Equations (Santiago de Compostella, 1987)*, 208–212. Springer-Verlag, Berlin, 1989.

[11] S. Osher, J. Sethian. Fronts propagating with curvature dependent speed: algorithms based on Hamilton–Jacobi formulations. *J. Comput. Phys.*. **79**: 12–49, 1988.

[12] J. Sethian. *Level Set Methods and Fast Marching Methods.* Cambridge University Press, Cambridge, 1999.

[13] J. Sokolowski, J-P. Zolesio. *Introduction to Shape Optimization.* Springer-Verlag, Berlin, 1992.

[14] M. Sussman, P. Smereka, S. Osher, A level set method for computing solutions to incompressible two-phase flow. *J. Comput. Phys.*, **114**: 146–159, 1994.